2020 IEEE International Conference on Robotics and Automation (ICRA)
31 May - 31 August, 2020. Paris, France

Interconnection and Damping Assignment Passivity-Based Control for Gait Generation in Underactuated Compass-Like Robots

Pierluigi Arpenti, Fabio Ruggiero, Vincenzo Lippiello

***Abstract*— A compass-like biped robot can go down a gentle slope without the need of actuation through a proper choice of its dynamic parameter and starting from a suitable initial condition. Addition of control actions is requested to generate additional gaits and robustify the existing one. This paper designs an interconnection and damping assignment passivity-based control, rooted within the port-Hamiltonian framework, to generate further gaits with respect to state-of-the-art methodologies, enlarge the basin of attraction of existing gaits, and further robustify the system against controller discretization and parametric uncertainties. The performance of the proposed algorithm is validated through numerical simulations and comparison with existing passivity-based techniques.**

I. Introduction

Passive dynamic walking is the stable gait performed by an unactuated biped robot, with a proper choice of the parameters, descending a moderate slope under the effect of the gravitational field. Firstly investigated in [1], this phenomenon emerges when an inelastic impact with the ground dissipates the kinetic energy gain at the end of every single step, resetting the potential energy to its initial value. If both the robot and the environment meet particular geometrical and inertial conditions, the mechanical (total) energy of the biped is constant during each step, and thus the whole process evolves indefinitely. A limit-cycle represents such behavior in the phase plane of the robot state variables. The interest in studying passive dynamic walking is twofold. As first, passive walking exhibits similarities with human gait features, serving as a testbed to investigate human locomotion [2]. Secondly, this kind of motion is energetically efficient compared to the other state-of-the-art biped locomotion control strategies based on walking primitives preplanning and on the zero moment point stability criterion [3]. Since such a passive gait is naturally exhibited by the unactuated biped robot when the initial conditions are precisely on the associated limit cycle, adding a control action is useful for two reasons. The former is the possibility to enlarge the basin of attraction of the passive gait. The latter is the possibility to generate additional gaits to the original one exhibited without actuation. Therefore, studying passive dynamic walking can be the starting point to develop energy-saving control strategies.

A broad overview about how generic legged robots are modeled and how they are controlled is given in [4]. In particular, a mix between mechanical design and learning algorithms is used in [5] to find an efficient control policy. A passive dynamic for a multiple degrees of freedom underactuted biped is generated in [6] by combining a passive controller and a proportional-derivative one.

This work focuses on a specific passive walker, the compass-like biped robot (CBR) which, despite its simple kinematic structure, exhibits a very complicated dynamic behavior due to the hybrid nature of the system [7]. An effective, but still poorly used, strategy to control the CBR is the energy shaping [8] which represents a dominant class of methodologies able to exploit the intrinsic passive nature of such a type of systems. Most of the works proposed in the literature derive the control laws starting from a Lagrangian modelling framework. For example, a potential energy shaping finalized to make the biped's gait slope invariant is applied in [9]. A potential energy shaping is instead employed in [10] to regulate the biped's forward walking speed. Besides, a total energy shaping approach enlarges the basin of attraction of the limit cycle, increases the rate of convergence, and makes the gait more robust over uncertainties on the initial conditions. The former cited works [9] and [10] consider a fully actuated biped robot model. However, studies on the natural human gait show that the primary energy source for the forward motion comes from ankles and that an ankle-only actuation is more energetically efficient than a hip-only one. These biomechanical considerations are explained in [11], motivating a kinetic energy shaping control for an underactuated CBR which creates new walking gaits based on the controlled Lagrangian methodology [12], [13]. Starting from the port-Hamiltonian (pH) modelling framework, a similar result is achieved in [3] where the proposed control strategy is based on the interconnection and damping assignment passivity-based control (IDA-PBC) [14], [15], that is capable to generate robust gaits characterized by small step lengths and slow forward speed. In particular, the methodology followed in [3], based on [16], requires that the open loop inertia matrix does not depend on actuated generalised coordinates, forcing the authors to perform a preliminary change of coordinates to get a suitable dynamic model. Other energy-efficient control approaches which exploit the pH framework are proposed in [17] for several walking robots.

This paper proposes a further methodology to control an

The research leading to these results has been supported by the PRINBOT project (in the frame of the PRIN 2017 research program, grant number 20172HHNK5_002); the WELDON project (in the frame of Programme STAR, financially supported by UniNA and Compagnia di San Paolo); the AERIAL-CORE project (Horizon 2020, Grant Agreement No.871479). The authors are solely responsible for its content.

Authors are with the PRISMA Lab, Department of Electrical Engineering and Information Technology, University of Naples, Via Claudio 21, 80125, Naples, Italy. Contact emails {pierluigi.arpenti, fabio.ruggiero, vincenzo.lippiello}@unina.it

underactuated CBR through the IDA-PBC, without solving the partial differential equations that usually characterize such a control methodology, and without requiring any change of coordinates as in [3], since the method applies to systems with inertia matrices depending on both actuated and unactuated coordinates. The proposed control law takes inspiration from [18], where the holonomic rolling primitive of nonprehensile manipulation is solved, and [19], where the same methodology is applied to a benchmark system like the translational oscillator with a rotational actuator system.

The contributions of this work are numerous. i) The proposed methodology is a suitable adaptation of [18] applied to the robotic legged domain, confirming that there exists a connection between nonprehensile manipulation and legged systems as sketched out in [20]: this may open new scenarios for the control design in both domains. ii) The proposed methodology, by suitably tuning the gains, can generate additional gaits to state-of-the-art control designs. iii) The basin of attraction of existing gaits can be increased. iv) The proposed methodology is robust to the discretization of the controller and parametric uncertainties.

II. IDA-PBC In a Nutshell

The pH mathematical model of a planar and underactuated mechanical system (i.e., with $n=2$ state variables and $m=1$ control input), neglecting system natural damping, is

$$\begin{bmatrix}\dot{q}\\ \dot{p}\end{bmatrix} = \begin{bmatrix}O_2 & I_2\\ -I_2 & O_2\end{bmatrix}\nabla H(q,p) + \begin{bmatrix}0_2\\ G\end{bmatrix}u, \tag{1}$$

where $q = \begin{bmatrix}q_1 & q_2\end{bmatrix}^T \in \mathbb{R}^2$ is the vector of generalised coordinates, $p = \begin{bmatrix}p_1 & p_2\end{bmatrix}^T \in \mathbb{R}^2$ is the vector of generalised momenta, $I_2 \in \mathbb{R}^{2\times 2}$ is the identity matrix, $O_2 \in \mathbb{R}^{2\times 2}$ is the null matrix, $0_2 \in \mathbb{R}^2$ the zero vector, $G = \begin{bmatrix}1 & 0\end{bmatrix}^T \in \mathbb{R}^2$ the input mapping term, and $u \in \mathbb{R}$ is the control input. The scalar function $H : \mathbb{R}^4 \to \mathbb{R}$ is the Hamiltonian expressing the total (mechanical) energy (kinetic plus potential) stored in the system, whose expression is

$$H(q,p) = \frac{1}{2}p^T M^{-1}(q)p + V(q), \tag{2}$$

where $V(q) \in \mathbb{R}$ is the potential energy and $M(q) \in \mathbb{R}^{2\times 2}$ is the positive-definite mass matrix whose elements are $b_{i,j}(q)$, with $i,j = \{1,2\}$.

The IDA-PBC is a passivity-based control methodology which shapes the total energy in such a way that it has a minimum in the desired equilibrium for the closed-loop system. Moreover, the control assures the asymptotic stability of the desired equilibrium by a damping injection if the passive output is detectable [14]. The IDA-PBC consists of finding a control law such that the closed-loop dynamics match a target pH system with dissipation through the following equations

$$\begin{bmatrix}\dot{q}\\ \dot{p}\end{bmatrix} = \begin{bmatrix}O_2 & M^{-1}(q)M_d(q)\\ -M_d(q)M^{-1}(q) & J_2(q,p) - Gk_dG^T\end{bmatrix}\nabla H_d(q,p), \tag{3}$$

where $k_d > 0$ is a positive damping gain, $M_d(q) \in \mathbb{R}^{2\times 2}$ is the desired mass matrix that must be symmetric and positive definite (***Condition 1***), while $H_d : \mathbb{R}^4 \to \mathbb{R}$ is the following desired closed-loop Hamiltonian

$$H_d(q,p) = \frac{1}{2}p^T M_d^{-1}(q)p + V_d(q), \tag{4}$$

with $V_d(q) \in \mathbb{R}$ the desired potential energy such that $(q^*, 0_2) = \text{argmin } H_d(q,p)$ (***Condition 2***) in which $q^\star \in \mathbb{R}^2$ is the desired equilibrium, and $J_2(q,p) \in \mathbb{R}^{2\times 2}$ is the assigned interconnection skew-symmetric matrix (***Condition 3***). To ensure the sought match, a set of partial differential equations (PDEs) arise, which commonly are the bottleneck of this methodology. Let $G^\perp = \begin{bmatrix}0 & 1\end{bmatrix} \in \mathbb{R}^{1x2}$ be the left annihilator of G, these PDEs are

$$\begin{aligned}G^\perp(\nabla_q(p^T M^{-1}(q)p) - M_d(q)M^{-1}(q)\nabla_q(p^T M_d^{-1}(q)p)\\ + 2J_2(q,p)M_d^{-1}(q)p) = 0\end{aligned} \tag{5}$$

and

$$G^\perp(\nabla_q V(q) - M_d(q)M^{-1}(q)\nabla_q V_q) = 0, \tag{6}$$

called respectively *kinetic energy* and *potential energy matching equations* (KE-ME and PE-ME). Such matching equations must be solved for $M_d(q)$, $V_d(q)$, and $J_2(q,p)$ satisfying Conditions 1, 2, and 3. The energy shaping control law can be written as

$$\begin{aligned}u_{es} = (G^T G)^{-1}G^T(\nabla_q H(q,p)\\ - M_d(q)M^{-1}(q)\nabla_q H_d(q,p) + J_2(q,p)M_d^{-1}(q)p),\end{aligned} \tag{7}$$

stabilizing the closed-loop dynamics at the desired equilibrium $(q,p) = (q^\star, 0_2)$ thanks to the choice of $M_d(q)$, $V_d(q)$, and $J_2(q,p)$ as mentioned above. Moreover, in order to guarantee asymptotic stability of the equilibrium point, it is possible to inject a *damping term* expressed as $u_{di} = -k_d G^T \nabla_p H_d(q,p)$. The sought IDA-PBC law is $u = u_{es} + u_{di}$ which, as expected, assigns the desired target dynamic (3) to the system (1). Further details about pH systems, IDA-PBC and its application to underactuated mechanical systems can be found in [14] and [21].

A novel control strategy avoiding the explicit solutions of the PDEs is presented in [18]. The following ad-hoc parameterization of the closed-loop inertia matrix

$$M_d(q,c_1) = \begin{bmatrix}m_{11}(q,c_1) & m_{12}(q,c_1)\\ m_{12}(q,c_1) & m_{22}(q,c_1)\end{bmatrix}, \tag{8}$$

with $m_{i,j}(q,c_1) = \Delta a_{ij}(q,c_1) \in \mathbb{R}$, Δ is the determinant of $M(q)$, $a_{i,j}(q,c_1)$ is a generic function of its parameters, where $i,j = \{1,2\}$, and $c_1 \in \mathbb{R}^{n_{c1}}$ is a suitable set of gains to design the controller, yields the following PE-ME

$$\nabla_{q_2} V(q) + \alpha(q,c_1)\nabla_{q_1} V_d(q,c_2) + \beta(q,c_1)\nabla_{q_2} V_d(q,c_2) = 0 \tag{9}$$

where $c_2 \in \mathbb{R}^{n_{c2}}$ is an additional set of gains useful to design the controller, while $\alpha(q,c_1)$ and $\beta(q,c_1)$ are two scalar functions. These are defined as linear combination of the elements of $M(q)$ and $M_d(q,c_1)$ in such a way as the desired potential energy $V_d(q,c_2)$ can be computed without explicitly

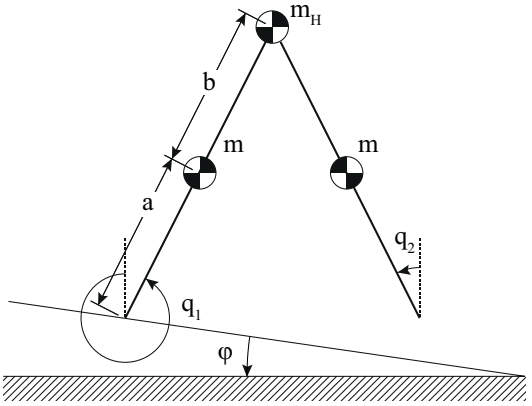

Fig. 1. Schematic representation of the CBR descending a slope and the related dynamic parmeters.

solving (9). Once $V_d(q,c_2)$ is found, $M_d(q,c_1)$ is computed and the KE-ME is solved as an algebraic equation. Finally, the control law u is designed as defined above. Further details on this approach can be found in [18].

III. The Compass-Like Biped Robot

The CBR is a planar biped composed by two legs joined by the hip [7]. Its motion is characterised, on determinate slopes, by a stable gait in the sagittal plane, without actuation and under the sole action of gravity.

The derived mathematical model only describes the swing motion of the nonsupporting leg before the impact with the ground. Afterward, the supporting and nonsupporting leg are swapped. Following [11], an underactuated compass-like biped robot (UCBR) is here addressed by supposing the actuation applied to the ankle of the supporting leg. Referring to Fig. 1, q_1 and q_2 are both measured with respect to the vertical. The angle q_1 is always referred to the support leg, while q_2 is always referred to the nonsupport one. Therefore, these angles are not associated to a physical leg, but they are referred to the action played by the leg during the gait.

The inertia matrix of the UCBR is given by

$$M(q) = \begin{bmatrix} (m_H+m)l^2+ma^2 & -mlb\cos(q_1-q_2) \\ -mlb\cos(q_1-q_2) & mb^2 \end{bmatrix}, \tag{10}$$

with $m_H > 0$ the hip mass, $m > 0$ the leg mass, $a > 0$ the distance between the foot and the leg mass, $b > 0$ the distance between the leg mass and the hip mass and $l = a+b$. The potential energy associated to the UCBR is given by

$$V(q) = g(m(a+l)+m_H l)\cos(q_1) - gbm\cos(q_2), \tag{11}$$

where $g > 0$ is the gravity acceleration. The pH mathematical model of the UCBR is then defined as in (1). As mentioned above, the UCBR exhibits an hybrid dynamic consisting in a swing phase plus an impact phase. An impact occurs when

$$\begin{aligned} y_h(q) &= l[\cos(q_1+\varphi) - cos(q_2+\varphi)] = 0 \\ \dot{y}_h(q) &= l[\sin(q_2+\varphi)\dot{q}_2 - sin(q_1+\varphi)\dot{q}_1] < 0 \end{aligned} \tag{12}$$

where $\varphi > 0$ is the slope of the ground and $y_h \in \mathbb{R}$ is the distance between the nonsupporting foot and the ground. Assuming a plastic and non slipping contact between legs and ground, as well as an instantaneous transfer from supporting to nonsupporting one (no double-support phase admitted), the impact causes this instantaneous change

$$\dot{q}(t^+) = P(q(t^-))\dot{q}(t^-), \tag{13}$$

where $\dot{q} = \begin{bmatrix} \dot{q}_1 & \dot{q}_2 \end{bmatrix}^T$ is the velocity vector, t^- and t^+ indicate the time instants just before and just after the impact event, respectively. The mapping matrix $P(q(t^-)) \in \mathbb{R}^{2\times 2}$ is obtained applying the law of conservation of angular momentum and it is not reported here for space constraints [7]. The gait exhibited by the UCBR endows a left-right symmetry, hence the angles q_1 and q_2 are swapped and relabeled at each impact, i.e. when an impact occurs, the former nonsupport leg becomes the support one and vice-versa [3]. It must be underscored that such kind of robot is not physically realizable due to the scuffing between the nonsupport foot and the the ground. In real prototypes foot scuffing is avoided by particular mechanical designs, as the one proposed in [22], whereas in this paper it is avoided by ignoring (12) whenever the nonsupport leg is behind the support one [11].

IV. IDA-PBC Design for the Underactuated Compass-like Robot

The purpose of this work is to create gaits different from the passive one employing the control action. The control strategy is a suitable modification of the procedure presented in [18], and synthetically recapped in Section II.

Considering the pH mathematical model of the UCBR presented in the previous section and the procedure illustrated in Section II, the desired inertia matrix parameterization (8) leads to the PE-ME as in (9). The crucial step is the choice of $\alpha(q,c_1)$ and $\beta(q,c_1)$ functions. Selecting $\alpha(q,c_1) = 0$ and $\beta(q,c_1) = -1/k_1^2$, with $k_1 \in \mathbb{R}$ a suitable gain, yields the following explicit solution for (9)

$$V_d(q,k_1,k_2) = k_2 g(am + l(m+m_H))\cos(q_1) - k_1 bmg\cos(q_2), \tag{14}$$

with $k_2 \in \mathbb{R}$ an additional gain. In order to obtain the solution (14), the interested reader can refer to the Case 3 of the Appendix in [18].

The potential energy shaping stage of the IDA-PBC requires to assign a closed-loop potential energy with the minimum at a desired equilibrium. Notice that (14) has exactly the same structure of (11). The two gains k_1 and k_2 weight the components of the open loop potential energy relative to the nonsupporting and the supporting leg, respectively. Since the UCBR without the impact resembles a double inverted pendulum, the most natural choice seems to assign as equilibrium $q^* = \begin{bmatrix} \pi & 0 \end{bmatrix}^T$ which is the same of the open loop mathematical model. The gradient vector of V_d is

$$\nabla_q V_d(q,k_1,k_2) = \begin{bmatrix} -gk_2(am + l(m+m_H))\sin(q_1) \\ bgk_1 m\sin(q_2) \end{bmatrix}. \tag{15}$$

Evaluating both (15) and the Hessian $\nabla_q^2 V_d(q,k_1,k_2)$ at q^*, results in a null gradient vector, whatever the values of the

gains k_1 and k_2 are, and in a definite positive Hessian matrix if $k_1, k_2 > 0$. Hence, Condition 2 is fulfilled with $k_1, k_2 > 0$.

From [18], recalling the chosen functions $\alpha(q, c_1)$ and $\beta(q, c_1)$, the elements of the desired inertia matrix (8) can be retrieved as

$$m_{12}(q, c_1) = \frac{b_{12}(q)}{k_1^2}, \quad m_{22}(q, c_1) = \frac{b_{22}(q)}{k_1^2}, \tag{16}$$

while, differently from [18], $m_{11}(q, c_1)$ is left free as

$$m_{11}(q, c_1) = k_3 \frac{k_4 \Delta + k_6 f(q) b_{12}(q)^2}{k_5 \Delta + k_6 f(q) b_{22}(q)}, \tag{17}$$

with $f(q) \in \mathbb{R}$ a function to be selected, and $k_3, k_4, k_5, k_6 \in \mathbb{R}$ some gains. The desired inertia matrix is then computed as (8). To fulfill Condition 1, $M_d(q, c_1)$ must be positive definite. Through the Sylvester criterion, this is satisfied by proper choices of the function $f(q)$ as well as of the gains for each of the case studies. In particular, both $m_{1,1}(q, c_1) > 0$ and $\Delta_d > 0$, with Δ_d the determinant of $M_d(q, c_1)$, must hold.

Finally, the interconnection matrix is chosen as

$$J_2(q, p) = \begin{bmatrix} 0 & j_2(q, p) \\ -j_2(q, p) & 0 \end{bmatrix}, \tag{18}$$

that is structurally skew-symmetric fulfilling Condition 3. The scalar function $j_2(q, p) \in \mathbb{R}$ is computed as in [18]

$$j_2(q, p) = \left(2 G^T M_d^{-1}(q, c_1) p\right)^{-1} \Big(G^{\perp} \nabla_q \left(p^T M^{-1}(q) p\right) - G^{\perp} M_d(q, c_1) M^{-1}(q) \nabla_q \left(p^T M_d^{-1}(q, c_1) p\right) \Big). \tag{19}$$

Due to space constraints, the explicit value of (19) is not displayed. However, it is possible to show that such a term is not affected by any singularity as instead highlighted in [18]. This peculiarity opens to new possibilities as sketched out in Section VI. Finally, the energy shaping control law (7) can be computed. To be more rigorous, the stability of the limit cycle arising from the impact between the biped and the ground should be assessed through Poincaré map method or via constructive tools as the one proposed in [23] for the orbital stabilization of underactuated nonlinear systems, but this is left as future work.

V. Case Studies

In this section, three different case studies are proposed and the relative numerical simulations are performed to test the ability of the controller in generating new gaits as well as to evaluate the robustness respect to parametric uncertainties. A comparison with the gaits generated in [11] is carried out.

The chosen model parameters are $m_H = 10$ kg, $m = 5$ kg, $a = 0.5$ m, $b = 0.5$ m, $g = 9.8$ m/s^2, and $\varphi = 3$ deg. Two parameters are introduced to describe a gait, namely the step length S and the period T. The former is the step length evaluated every two foot-ground impacts, while the latter is the duration of each single step.

The simulations are carried out in the MATLAB environment on a standard personal computer, and they last 30 s. The dynamic model of the UCBR (1) is numerically simulated through the *ODE*45 function of MATLAB with the event detection option active so as to evaluate the hit with the ground. The designed controller is implemented at a discrete time step of 0.01 s. A video displaying the obtained gaits is available as a multimedia attachments.

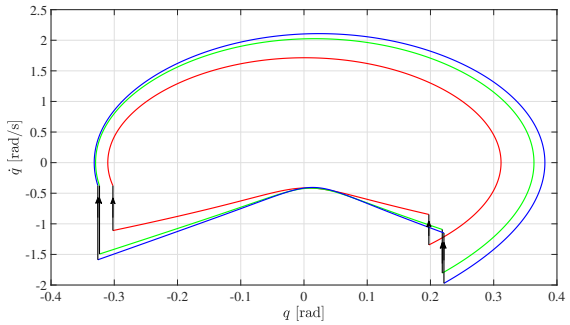

Fig. 2. Case Study 1. Three different limit cycles during a test carried out in nominal conditions. Green limit cycle represents the passive gait. Red and blue limit cycles are generated varying k_1 and k_2. The black arrows indicate the evolution of the state trajectories in forward time. The top arcs represent the evolution of q_2, while the bottom ones represent the evolution of q_1 in an entire gait. The black vertical axes indicate the discontinuities caused by an impact with the ground.

A. Case Study 1

This first case study shows the possibility of generating new stable gaits, compared to the passive gait naturally exhibited by the UCBR, by suitably tuning the controller gains. Three different set of gains are tested. The following gains are kept fixed $k_4 = b_{11} = 16.25$, $k_5 = 1$, and $k_6 = k_d = 0$ while $k_3 = 1/k_1$. This choice yields $m_{11}(q, k_1) = b_{11}/k_1 > 0$, and $\Delta_d = b_{11}(q) b_{22}(q)/k_1^2 - b_{12}(q)^2/k_1^2$. Substituting (10), it becomes

$$\Delta_d = \frac{a^2 b^2 m^2 + b^2 l^2 m^2 + b^2 l^2 m \; m_H - b^2 l^2 m^2 \cos(q_1 - q_2)^2}{k_1^2} \tag{20}$$

which is always positive because $0 \leq b^2 l^2 m^2 (1 - \cos^2(q_1 - q_2)) \leq b^2 l^2 m^2$. Hence, the desired inertia matrix is definite positive because both $m_{11}(q, k_1) > 0$ and $\Delta_d > 0$. Therefore, Condition 1 is satisfied.

The tuning of the gains k_1 and k_2, directly involved in the potential energy shaping, are shown in Fig.2. This figure is obtained fixing k_4, k_5, and k_6 and trying to isolate the effect of the potential energy shaping on the final gait. Differently from [11] and [3], where only a kinetic energy shaping controller is implemented, here the total energy shaping results in a sharp variation of the closed-loop gait. The choice $k_1 = 0.85$ with $k_2 = 1$ creates the blue limit cycle in Fig.2, while $k_1 = 1.2$ and $k_2 = 0.5$ the red limit cycle in Fig.2. These differ from the passive limit cycle obtained with the controller turned off, which is equivalent to set $k_1 = 1$ and $k_2 = 1$ (green limit cycle in Fig.2).

B. Case Study 2

This case study shows the capability of the controller to generate both symmetric small gaits and symmetric big gaits, improving what obtained in [11] and [3].

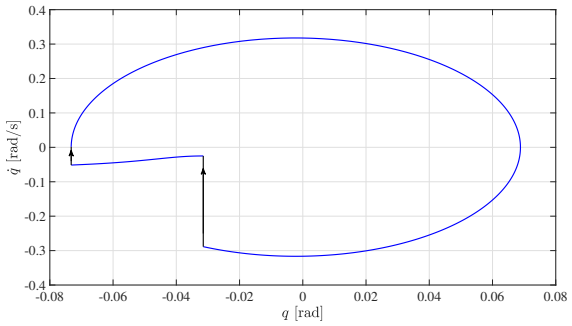

Fig. 3. Case Study 2, Small Gait. Limit cycle during a test carried out with nominal conditions.

Small Gait. The first simulation generates a slow symmetric gait characterized by a small step and a big period.

The gains are experimentally tuned as $k_1 = 1.1$, $k_2 = 1$, $k_3 = 1/k_1$, $k_4 = 0.04$, $k_5 = 0$, $k_6 = 1$, and $k_d = 0.1$. The function $f(q)$ in (17) is chosen equal to 1 yielding

$$m_{11}(q,k_3,k_4) = k_3 \frac{k_4\Delta + b_{12}(q)^2}{b_{22}} > 0. \tag{21}$$

After some calculations, Δ_d is equal to $k_4\Delta/k_1^2 > 0$. The Condition 1 is thus fulfilled and the resulting controller is similar to the one proposed in [3], apart from the potential energy shaping stage and the damping injection. The designed controller leads to a symmetric gait with $S = 0.0417$ m and $T = 1.149$ s, which is slower than the slowest symmetric one proposed in [3] having $S = 0.2012$ m and $T = 0.9996$ s. The gait parameters S and T converge to these very small values as in Fig.4, implying the crouched limit cycle of Fig.3.

Large Gait. Complementary to the previous test, now the goal is the generation of large and fast steps. For this task, $f(q) = \sin(q_1 - q_2)$ which transforms (17) into

$$m_{11} = k_3 \frac{k_4 b_{11} b_{22} - b_{12}^2(k_4 - k_6 \sin(q_1 - q_2))}{k_5(b_{11}b_{22} - b_{12}^2) + k_6 \sin(q_1 - q_2) b_{22}}, \tag{22}$$

where dependencies are suppressed and $k_i > 0$, with $i = \{3,4,5,6\}$. Folding (10) into the numerator of (22), called m_{11n}, yields $m_{11n} = a^2b^2k_4m^2 + b^2k_4l^2m^2(1 - \cos^2(q_1 - q_2)) + b^2k_4l^2mm_H + b^2k_6l^2m^2\cos^2(q_1 - q_2)\sin(q_1 - q_2)$. Since $0 \leq b^2k_4l^2m^2(1 - \cos^2(q_1 - q_2)) \leq b^2k_4l^2m^2$, it is possible to write $m_{11n} \geq (a^2m + m_H)b^2mk_4 + b^2k_6l^2m^2\cos^2(q_1 - q_2)\sin(q_1 - q_2) \geq (a^2m + m_H)b^2mk_4 - b^2k_6l^2m^2$. Therefore, $m_{11n} > 0$ if $k_6 < (a^2m + m_H)k_4/l^2$. On the other hand, using (10), the denominator of (22) is $m_{11d} = a^2b^2k_5m^2 + b^2k_5l^2mm_H + b^2k_5l^2m^2(1 - \cos^2(q_1 - q_2)) + b^2k_6m\sin(q_1 - q_2)$. Since $0 \leq b^2k_5l^2m^2(1 - \cos^2(q_1 - q_2)) \leq b^2k_5l^2m^2$, it is possible to write $m_{11d} \geq (a^2m + l^2m_h)b^2mk_5 + b^2k_6m\sin(q_1 - q_2) \geq (a^2m + l^2m_h)b^2mk_5 - b^2k_6m$. Therefore, $m_{11d} > 0$ if $k_6 < k_5(a^2m + l^2m_H)$. In conclusion, to assure $m_{11} > 0$ it is sufficient to choose the gain k_6 such as both $k_6 \leq (a^2m + m_H)k_4/l^2$ and $k_6 < k_5(a^2m + l^2m_H)$. The case of both $m_{11n} < 0$ and $m_{11d} < 0$ was not considered, and thus the found solution is conservative.

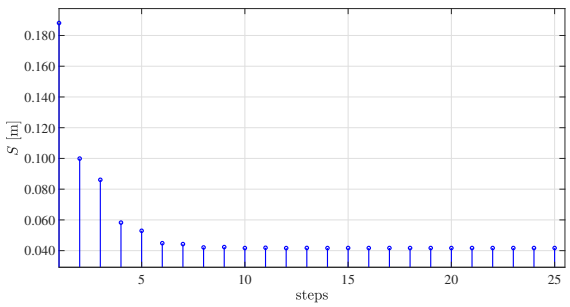

(a) Time history of S.

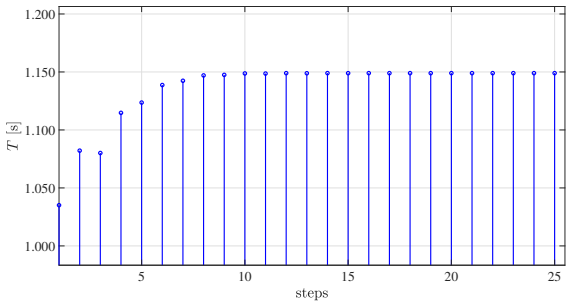

(b) Time history of T.

Fig. 4. Case Study 2, Small Gait. Time histories of the gait parameters.

To ease the computations, selecting $k_3 = 1/k_1$ and $k_5 = 1$ yields

$$\Delta_d = \frac{\Delta(b_{22}k_4 - b_{12}^2)}{k_1^2(\Delta + b_{22}k_6\sin(q_1 - q_2))}. \tag{23}$$

Folding (10) into the numerator of Δ_d yields $\Delta_{dn} = \Delta(mb^2k_4 - m^2l^2b^2\cos^2(q_1 - q_2)) \geq \Delta(mb^2k_4 - m^2l^2b^2)$. This is positive when $k_4 > ml^2$. On the other hand, using (10), the denominator of (23) is $\Delta_{dd} = k_1^2(m_Hl^2mb^2 + m^2b^2l^2 + m^2a^2b^2 - m^2l^2b^2\cos^2(q_1 - q_2) + mb^2k_6\sin(q_1 - q_2))$. Since $0 \leq m^2l^2b^2(1 - \cos^2(q_1 - q_2)) \leq m^2l^2b^2$, it is possible to write $\Delta_{dd} \geq k_1^2(m_Hl^2mb^2 + m^2a^2b^2 + mb^2k_6\sin(q_1 - q_2)) \geq k_1^2(m_Hl^2mb^2 + m^2a^2b^2 - mb^2k_6)$. This is positive when $k_6 < m_Hl^2 + ma^2$. In conclusion, to assure $\Delta_d > 0$ it is sufficient choosing $k_4 > ml^2$ and $k_6 < m_Hl^2 + ma^2$. The case of both $\Delta_{dn} < 0$ and $\Delta_{dd} < 0$ was not considered.

To recap, with the choice $k_3 = 1/k_1$ and $k_5 = 1$, Condition 1 holds when $k_6 < m_Hl^2 + ma^2$, $k_6 \leq (a^2m + m_H)k_4/l^2$, and $k_4 > ml^2$ are all fulfilled.

Hence, the selected gains ensuring Condition 1 are $k_1 = 1.7$, $k_2 = 1$, $k_3 = 0.588$, $k_4 = b_{11} = 16.25$, $k_5 = 1$, $k_6 = 6.2$, and $k_d = 0$. The simulation shows the generation of a symmetric gait characterised by $T = 0.6806$ s and $S = 0.8738$ m, as depicted in Fig. 6. This gait is faster than the one in [11] ($T = 0.7118$ s, $S = 0.7784$ m). The two controllers are compared in Fig. 5 where it is visible that the area of the cycle limit obtained through the controlled Lagrangian (CL) method in [11] is almost totally contained by the area of limit cycle generated by the proposed approach.

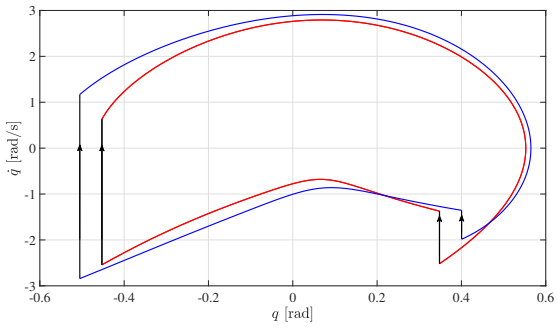

Fig. 5. Case Study 2, Large Gait. Limit cycles during a test carried out with nominal conditions. In blue, the gait generated with the proposed IDA-PBC approach. In red the gait generated with the CL method.

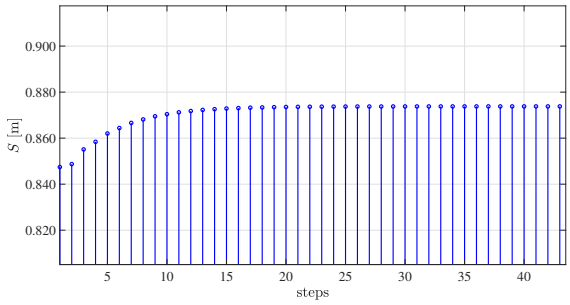

(a) Time history of S.

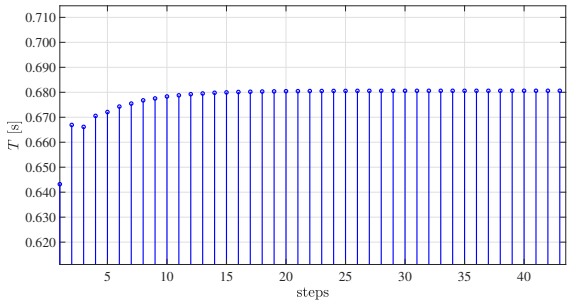

(b) Time history of T.

Fig. 6. Case Study 2, Large Gait. Time histories of the step length and the step period during a test carried out with nominal conditions.

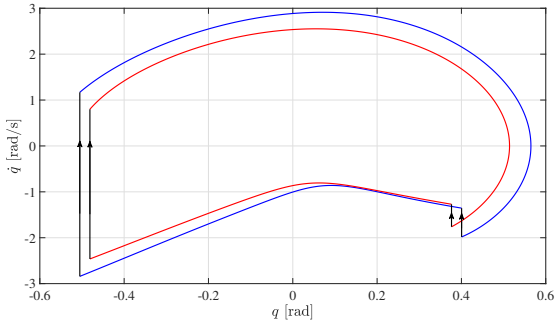

Fig. 7. Case Study 3, Large Gait, Parametric Uncertainty. Limit cycle during a test carried out with a 10% uncertainty on both masses and lengths. In blue, the large gait generated form Case Study 2, without any parametric uncertainty. In red, the gait generated with the same controller and with the same gains, in presence of parametric uncertainty.

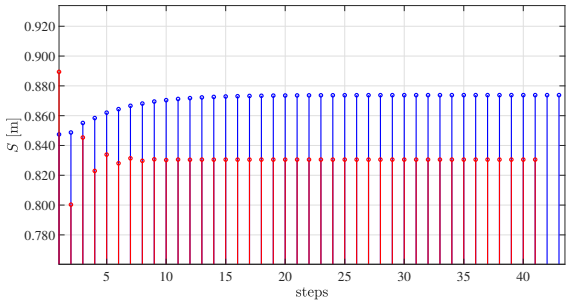

(a) Time history of S.

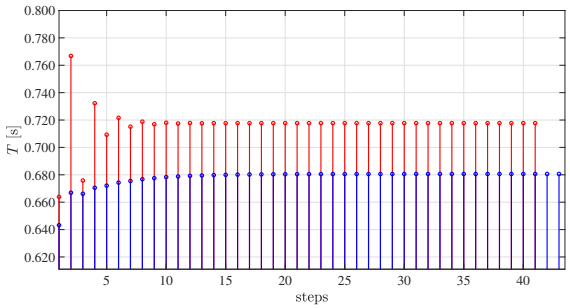

(b) Time history of T.

Fig. 8. Case Study 3, Large Gait, Parametric Uncertainty. Time histories of S and T during a test carried out with a 10% uncertainty on both masses and lengths. In blue, the gait without any parametric uncertainty. In red, the same gait with uncertainty. The UCBR with parametric uncertainties results to be slower since it performs 41 steps versus the 43 steps of the UCBR without parametric uncertainties within the same simulation time.

C. Case study 3

The proposed controller is also robust with respect to parametric uncertainties. In particular, this is designed on the nominal values of the dynamic parameters, while the ODE45 function simulating the system dynamics sees an increment of 10% for the masses and the lengths of the UCBR.

A different, but symmetric, gait is generated with the same gains proposed in the Case Study 2 for the generation of large and fast steps. The gait parameters time histories testify the robustness of the approach as showed in Fig.8. It is possible to notice that the gait is symmetric and also it is very close to the gait obtained in case of perfect knowledge of the inertial and kinematic parameters of the system as depicted in Fig.7.

VI. Conclusion and Future Work

An IDA-PBC was designed in this paper for an UCBR. The objective of the work was to generate further gaits with respect to available state-of-the-art methodologies and robustify the system against uncertainties. Numerical simulations and comparisons validated the approach. Future work will be twofold. Form a theoretical point of view, it would be interesting investigating how to solve the numerical singularity affecting [18] by generalizing the solution found in this paper for the biped system. Besides, it would be challenging to apply the proposed approach to a biped robot with more degrees of freedom than a compass-like robot.

REFERENCES

[1] T. McGeer, "Passive dynamic walking," *International Journal of Robotic Research*, vol. 9, no. 2, pp. 62–82, 1990.

[2] A. Kuo, "The six determinants of gait and the inverted pendulum analogy: A dynamic walking perspective," *Human Movement Science*, vol. 26, no. 4, pp. 617–656, 2007.

[3] V. De-León-Gómez, V. Santibanéz, and J. Sandoval, "Interconnection and damping assignment passivity-based control for a compass-like biped robot," *International Journal of Advanced Robotic Systems*, vol. 14, no. 4, 2017.

[4] P.-B. Wieber, R. Tedrake, and S. Kuindersma, "Modeling and control of legged robots," in *Springer Handbook of Robotics*, B. Siciliano and O. Khatib, Eds. Springer International Publishing, 2016, pp. 1203–1234.

[5] S. Collins, A. Ruina, R. Tedrake, and M. Wisse, "Efficient bipedal robots based on passive dynamic walkers," *Science,*, vol. 307, pp. 1082–1085, 2005.

[6] M. Yeatman, G. Lv, and R. Gregg, "Passivity-based control with a generalized energy storage function for robust walking of biped robots," in *Annual American Control Conference*, Milwaukee, USA, 2018.

[7] A. Goswami, B. Thuilot, and B. Espiau, "Compass-like biped robot Part I: Stability and bifurcations of passive gaits," *Institut National de Recherche en Informatiqu et en Automatique (INRIA),Techical Report 2996*, 1996.

[8] K. Fujimoto and S. Toshiharu, "Canonical transformations and stabilization of generalized Hamiltonian systems," *System & Control Letters*, vol. 42, pp. 217–227, 2001.

[9] M. Spong and F. Bullo, "Controlled symmetries and passive walking," in *Proceeding IFAC Triennal World Congress*, Barcelona, Spain, 2002.

[10] M. Spong, J. Holm, and D. Lee, "Passivity-based control of bipedal locomotion," in *IEEE Robotics & Automation Magazine*, vol. 12, no. 2, 2007, pp. 30–40.

[11] J. Holm and M. Spong, "Kinetic energy shaping for gait regulation of underactuated bipeds," in *IEEE International conference on control applications*, San Antonio, Texas, USA, 2008, pp. 1232–1238.

[12] A. Bloch, N. Leonard, and J. Marsden, "Controlled lagrangians and the stabilization of mechanical systems. I. The first matching theorem," *IEEE Transactions on Automatic Control*, vol. 45, no. 12, pp. 2253–2270, 2000.

[13] A. Bloch, D. Chang, N. Leonard, and J. Marsden, "Controlled lagrangians and the stabilization of mechanical systems. II. Potential shaping," *IEEE Transactions on Automatic Control*, vol. 46, no. 10, pp. 1556–1571, 2000.

[14] R. Ortega, A. Van Der Schaft, B. Maschke, and G. Escobar, "Interconnection and damping assignment passivity-based control of port-controlled Hamiltonian systems," *Automatica*, vol. 38, no. 4, pp. 585–596, 2002.

[15] R. Ortega, A. Van Der Schaft, I. Mareels, and B. Maschke, "Putting energy back into control," *IEEE Control Systems Magazine*, pp. 18–33, 2001.

[16] J. Acosta, R. Ortega, and A. Astolfi, "Interconnection and damping assignment passivity-based control of mechanical systems with underactuation degree one," *IEEE Transactions on Automatic Control*, vol. 50, pp. 1936–1955, 2005.

[17] V. Duindam, "Port-Based Modelling and Control for Efficient Bipedal Walking Robots," Ph.D. dissertation, Ph.D. Dissertation, University of Twente, 2006.

[18] D. Serra, F. Ruggiero, A. Donaire, L. Buonocore, V. Lippiello, and B. Siciliano, "Control of nonprehensile planar rolling manipulation: A passivity based approach," *IEEE Transactions on Robotics*, vol. 35, no. 2, pp. 317–329, 2019.

[19] P. Arpenti, D. Serra, F. Ruggiero, and V. Lippiello, "Control of the TORA system through the IDA-PBC without explicit solution of matching equations," in *2019 Third IEEE International Conference on Robotic Computing*, Naples, Italy, Italy, 2019.

[20] I. Ramirez-Alpizar, M. Higashimori, M. Kaneko, C. Dylan Tsai, and I. Kao, "Dynamic nonprehensile manipulation for rotating a thin deformable object: An analogy to bipedal gaits," *IEEE Transactions on Robotics*, vol. 28, no. 3, pp. 607–618, 2012.

[21] R. Ortega, M. Spong, F. Gómez-Estern, and G. Blankenstein, "Stabilization of a class of underactuated mechanical systems via interconnection and damping assignment," *IEEE Transactions on Automatic Control*, vol. 47, no. 8, pp. 1218–1233, 2002.

[22] P. Bhounsule, J. Cortell, and A. Ruina, "Design and control of Ranger: An energy-efficient, dynamic walking robot," *Adaptive Mobile Robotics*, pp. 441–448, 2012.

[23] A. Shiriaev, L. Freidovich, and S. Gusev, "Transverse linearization for controlled mechanical systems with several passive degrees of freedom," *IEEE Transactions on Automatic Control*, vol. 55, no. 4, pp. 893–906, 2010.